Edge States and Topology in Floquet Systems

Ben Foutty
Department of Physics, Stanford University, Stanford, CA 94305
(Dated: June 20, 2020)

Submitted as coursework for PH470, Stanford University, Spring 2020

A detailed theoretical understanding of topological phases of matter is a key development in condensed matter physics over the last 40 years. As periodically driven, Floquet systems gain widespread interest, a logical question is how these topological phases, as developed in a single-particle band theory, extend to quasiperiodic Floquet spectra. In particular, we focus in on how chiral edge states, due to nontrivial topology, can arise in Floquet systems. In approaching this problem, various models of Floquet condensed matter systems displaying edge states are discussed along with an appropriate bulk-boundary correspondence based on the winding number of a properly chosen time evolution operator, rather than simply the Chern numbers of the Floquet eigenstates. In addition, we consider the role that many-body effects play in realizing these Floquet topological phases in physical systems.

I. INTRODUCTION

Beginning with the theoretical understanding of the quantum Hall effect in the 1980s, topology and topological order has played an important role in modern condensed matter physics[1,2]. Nonlocal properties of ground states of certain systems, combined with the presence of an energy gap, allow for robust topological order that doesn't depend strongly on details such as sample size and composition. As this theoretical framework was developed around the quantum Hall effect, it led to the later hypothesis and discovery of nontrivial topological phases in more general classes of condensed matter systems, such as topological insulators in 2 and 3 dimensions and topological superconductivity. While electronic correlations are inevitable in any physically realizable system, many of these effects are most easily classified and understood through a single-particle (i.e. band theory) picture, upon which a more robust, many-body picture can be developed. In topological band theory, the definition of Chern numbers (below) and the bulk-boundary correspondence connects intrinsic properties of the bulk band structure and the existence of edge states on the boundary. These edge states are a measurable signature of topological order; in the case of topological insulators, for example, the existence of a topological insulating phase was first confirmed through measurements of these edge states[3].

Recently, theoretical interest has grown in condensed matter systems out of equilibrium. One way of achieving this is to give the Hamiltonian $H(t)$ explicit time dependence, so that energy is no longer conserved. This case of completely arbitrary time-dependence is general to the point that it can difficult to admit a theory that covers this entire class of Hamiltonians. A more restrictive case of time-dependence which allows for a richer theoretical understanding is that of Floquet systems, where the time dependence is periodic with period T, i.e. $H(t+nT) = H(t)$ for $n \in \mathbb{Z}$. This also holds relevance to many experimental systems in the lab, as optically pumping via lasers provides a time dependence of this form.

In Floquet systems, there's still a notion of energy bands, albeit with some subtlety. A natural question is how one might extend the notions of topological band theory and the bulk-boundary corresponse to a system that is periodically driven. In this paper, we review the work of Rudner et. al., "Anomalous Edge States and the Bulk-Edge Correspondence for Periodically Driven Two-Dimensional Systems," which generalizes the concept of edge states to the case of a Floquet system[4]. In Part II, we discuss some necessary background of topological order in static systems and develop some formalism around Floquet systems. In Part III, we review the theoretical understanding of chiral edge states in Floquet systems following Rudner et. al., before discussing relevance to some recent physical experiments and many-body generalizations in Part IV.

II. BACKGROUND

A. Topological order in static systems

Before defining their generalization in Floquet systems, we will set down the important concepts of topological order in the time-independent case, following the notes from Charles Kane in "Topological band theory and the

Z2 invariant"[5]. Assuming some underlying lattice, the eigenstates of the Hamiltonian from Bloch's theorem can be expressed as $|\psi(\mathbf{k})\rangle = e^{i\mathbf{k}\cdot\mathbf{r}}|u(\mathbf{k})\rangle$ where $|u(\mathbf{k})\rangle$ is periodic over the unit cell. These $|u(\mathbf{k})\rangle$ form eigenvectors of the Hamiltonian $H(\mathbf{k})$ which have corresponding eigenvalues $E_n(\mathbf{k})$ that form the "bands" of band theory. However, these $|u(\mathbf{k})\rangle$ are only defined up to a phase, the Berry phase $\phi(\mathbf{k})$,

$$|u(\mathbf{k})\rangle \to e^{i\phi(\mathbf{k})}|u(\mathbf{k})\rangle \tag{1}$$

Noting the similarity to a gauge transformation in electromagnetism, one can define a Berry connection

$$\mathbf{A} = -i\langle u(\mathbf{k})|\nabla_{\mathbf{k}}|u(\mathbf{k})\rangle \tag{2}$$

for which the curl of $\mathbf{A}$, defined as the Berry curvature $\mathcal{F} = \nabla \times \mathbf{A}$, is analagous to a magnetic field. For a closed loop in k-space, then, the Berry phase γ_c is well defined (i.e. gauge invariant)

$$\gamma_c = \oint_C \mathbf{A} \cdot d\mathbf{k} \tag{3}$$

A simple case of this is a two-level system $H(\mathbf{k}) = \mathbf{d}(\mathbf{k}) \cdot \boldsymbol{\sigma}$, for which the Berry phase is simply one half the solid angle swept out by $\hat{\mathbf{d}}(\mathbf{k})$ along a closed curve on a sphere. In general, one can define a topological invariant called a Chern number on a closed surface S that is given by

$$n = \frac{1}{2\pi}\int_S \mathcal{F} d^2\mathbf{k} \tag{4}$$

While this is certainly an integer in the spherical, two level case, it remains integral even in more general cases, analagous to the Gauss-Bonnet theorem.

If we take the closed surface S over which we evaluate the Chern number to be individual bands in the band structure separated by an energy gap, then due to an argument from Laughlin and Halperin, the Chern number of a single band defines the difference between the numbers of chiral edge modes above and below the band[2,6,7]. In the case of isolated, static bands, then, the net number of chiral states is given by the sum over the Chern number of all occupied bands. Evaluating the Chern numbers of all of the bands in the band structure is then sufficient for completely understanding the behavior of edge states, and nontrivial Chern numbers are required to observe chiral edge states.

B. Floquet formalism

Eigenstate solutions to a Hamiltonian that is invariant under discrete time translation as $H(t+T) = H(t)$ can be understood via Floquet's theorem analagously to Bloch's theorem for eigenstates invariant under discrete space translation. A general eigenstate $|\psi(t)\rangle$ can be decomposed as

$$|\psi(t)\rangle = e^{-i\varepsilon t}|\Phi(t)\rangle, \quad |\Phi(t+T)\rangle = |\Phi(T)\rangle \tag{5}$$

where quasienergy ε can be defined up to integer multiples of $\frac{2\pi}{T}$. Just as we can reduce to a single Brillouin zone in momentum space in the spatial case, we can take the quasienergy to be defined on a Brillouin zone $-\pi/T < \varepsilon < \pi/T$, so that the Floquet spectrum consists of a set of quasienergy bands $\{\varepsilon_n(\mathbf{k})\}$, where we assume spatial translation symmetry as well. This Brillouin zone for our Floquet band structure is periodic in quasienergy as well as momentum, providing a qualitative difference from the static case. Further, the eigenstates $\{|\Phi_n(k,t)\rangle\}$ do retain time dependence t, though that time dependence is periodic with period T. We can understand this also through the evolution operator $U(t)$. Because $|\psi(T)\rangle = e^{-i\varepsilon T}|\psi(0)\rangle$, the quasienergy comes directy from the eigenvalues of $U(T)$:

$$|\psi(T)\rangle = U(T)|\psi(0)\rangle = e^{-i\varepsilon T}|\psi(0)\rangle \tag{6}$$

Another way to put this is that $U(t)$ can be expressed as

$$U(t) = \phi(t)e^{-iH_F t}, \quad \phi(t) = \phi(t+T) \tag{7}$$

where H_F is a Floquet effective Hamiltonian which is equivalent (considered as a static Hamiltonian under time evolution by time T) to the more complicated time evolution dictated by $H(t)$.

III. EDGE STATES IN FLOQUET SYSTEMS

In extending the concept of chiral edge states to the Floquet band theory, it's quick to see that the situation is more subtle. It is possible to define a Chern number for each band, though it now it must be evaluated over the eigenstates at a single moment in time t. This is cleaned up by the finding that the Chern numbers of the Floquet bands do remain fixed over the period T, so specifying Chern numbers of each band at $t = 0$, over the eigenstates $\{|\Phi_n(k,0)\rangle\}$, is equivalent to any other point in time[4,8]. However, the periodicity in quasienergy suggests that the bottom of the lowest band is no longer isolated from the rest of the system; edge states between the bottom of the lowest band and the top of the highest band are possible. Such behavior would allow for chiral edge states even if the Chern number of each band is trivial: considering two bands with zero Chern number, there could be one edge state connecting the two bands through the middle of the quasienergy zone and another edge state (in the same direction) connecting the two bands around the periodic quasienergy boundary. The Chern numbers are both satisfied as zero as the bands have net zero edge states entering and exiting them, but the system admits chiral edge states in the gaps.

A recent review[9] chooses to categorize drives as Type I and Type II depending on whether static topological band theory applied to Floquet-Bloch band structure is sufficient to describe the edge states and topological features of the system. With a Type I drive, the effective

Hamiltonian H_F can be evaluated considering its Floquet band structure as if it was static. While this doesn't lead to qualitatively new physics, this is of great interest in terms of "engineering" new physics not present in the original (undriven) Hamiltonian[10]. For example, a system with topologically trivial band structure, with every Chern number equal to zero, can develop nonzero Chern bands and corresponding edge states arise. Alternatively, Type II drives lead to "anomalous" or "nontrivial" edge , which would not be accounted for if we considered the Floquet-Bloch band structure as if it was a static band structure, such as the example of two Chern zero bands with edge states connecting them described above. A deeper theoretical understanding of these anomalous edge states is the main focus of the paper by Rudner et. al.[4] and will be discussed in the following sections.

A. RLBL (Lattice) Model

Rudner et. al. construct a tight-binding model on a square lattice to illustrate the possibilites of both of these sort of edge states, referred to as the RLBL Model. In this model, we have a bipartite square lattice with tight-binding hopping coefficients that are varied in time. The Hamiltonian is given by

$$H(t) = \sum_{\mathbf{k}} \begin{pmatrix} c^\dagger_{\mathbf{k},A} & c^\dagger_{\mathbf{k},B} \end{pmatrix} H(\mathbf{k},t) \begin{pmatrix} c_{\mathbf{k},A} \\ c_{\mathbf{k},B} \end{pmatrix},$$

$$H(\mathbf{k},t) = -\sum_{n=1}^{4} J_n(t)(e^{i\mathbf{b}_n\cdot\mathbf{k}}\sigma^+ + e^{-i\mathbf{b}_n\cdot\mathbf{k}}\sigma^-) + \delta_{ab}\sigma_z. \quad (8)$$

Here the $c^\dagger_{\mathbf{k},A/B}$ are the usual Bloch creation operators with momentum $\mathbf{k}$ on the A/B sublattice and the vectors $\mathbf{b}_i$ are given by the lattice vectors $\mathbf{b}_1 = -\mathbf{b}_3 = (a,0)$ and $\mathbf{b}_2 = -\mathbf{b}_4 = (0,a)$. The system is driven in such away that $J_n(t)$ is piecewise constant along $T/5$ cycles, where on the $n \in \{1,2,3,4\}$ cycles, J_n is set to value J and all others are set to zero. In step 5, only the σ_z term contributes as a "holding period." A schematic is provided in Fig. 1a. H is Floquet periodic and controls the hopping on each of the 4 bonds from an A site to a neighboring B site (and vice versa) for an equal period of time - this leads to a chirality inherent in the drive as driving as $1-2-3-\ldots$ is inequivalent to $5-4-3-\ldots$ due to hopping occuring in opposite directions around the plaquettes.

A simple set of parameters to demonstrate the edge physics in this problem are $J = \frac{2.5\pi}{T}$ and $\delta_{AB} = 0$. In this case, a particle will hop with probability 1 between neighboring sites on each unit of the cycle. Thus, in an infinite system, every particle will simply hop around its plaquette and will be left as before. More technically, if we express H_i to be the Hamiltonian on each of the time steps, then $U(T) = e^{-iH_5T/5}e^{-iH_4T/5}\ldots e^{-iH_1T/5}$ reduces immediately to $\mathbf{1}$, corresponding with an effective Hamiltonian $H_F = 0$, completely trivial. However, the edge physics are a little more complicated, as a full plaquette cycle cannot be completed off of an edge and the resulting hopping will be only laterally along the edge.

To investigate the edge effects, we can solve numerically for the Floquet spectrum on a strip geometry. Setting a finite number of sites M in the y-direction, we express the Hamiltonian within each $T/5$ timestep as a $2M \times 2M$ matrix corresponding to the hopping in real-space along the y-axis and momentum $k_\parallel$ (and sublattice degree of freedom) along the x direction. By solving for the stationary states of $U(T) = e^{-iH_5T/5}e^{-iH_4T/5}\ldots e^{-iH_1T/5}$, we can find the quasienergy spectrum via Eq. 6 above. Applying these numerics to $J = \frac{2.5\pi}{T}$ and $\delta_{AB} = 0$ with a width of 30 sites along the y direction, we solve for the Floquet spectrum, seen in Fig. 1b. Nearly all of the modes are completely flat at quasienergy $\varepsilon = 0$, as expected from the bulk $H_F = 0$. However, two linearly dispersing modes cross the Brillouin zone corrsponding to the two chiral edge modes described above.

Varying J along with $\delta_{AB} \neq 0$ yields a rich phase diagram. In Fig. 1c-e, we plot the calculated Floquet spectrum for $\delta_{AB} = 0.5\pi/T$ and $J = 0.5\pi/T,\ 1.5\pi/T,\ 2.5\pi/T$. For the smallest hopping (Fig. 1c), the two bands are completely isolated and no edge states are seen. At intermediate $J = 1.5\pi/T$, we can see a single edge state crossing at $\varepsilon = \frac{\pi}{T}$ but the gap at $\varepsilon = 0$ still completely open. This suggests that the Chern numbers of the Floquet-Bloch bands are $\mathcal{C} = \pm 1$ respectively, which can be confirmed by direct numerical calculation from the Floquet eigenstates in the infinite size system calculated at a particular time. This signifies a "Type I" topological phase, as edge states arise due to the drive causing nonzero Chern bands in the spectrum. In the largest hopping, we see edge states crossing at both $\varepsilon = 0$ and $\varepsilon = \frac{\pi}{T}$, so that both of our Floquet-Bloch bands have Chern numbers $\mathcal{C} = 0$ but there are "anomalous" chiral edge states nevertheless. The physics of this model motivate a bulk-boundary correspondence that's generalized to the Floquet case, which is established by Rudner et. al. and discussed in the following section. Application of this invariant predicts the correct number of edge states seen in the numerical solutions of the RLBL model.

B. Construction of invariant

Considering a tight binding model on a 2D lattice with an arbitrary number of sublattices, then the time-dependent Hamiltonian can be expressed as

$$H(t) = \sum_{\mathbf{k},\alpha,\alpha'} c^\dagger_{\mathbf{k},\alpha} H_{\alpha\alpha'}(\mathbf{k},t) c_{\mathbf{k},\alpha'} \quad (9)$$

Recognizing $H(\mathbf{k},t)$ as an $N \times N$ Hermitian matrix, the bulk time evolution operator is given by the Schrodinger equation as

$$U(\mathbf{k},t) = \mathcal{T} e^{-i\int_0^t dt' H(\mathbf{k},t')} \quad (10)$$

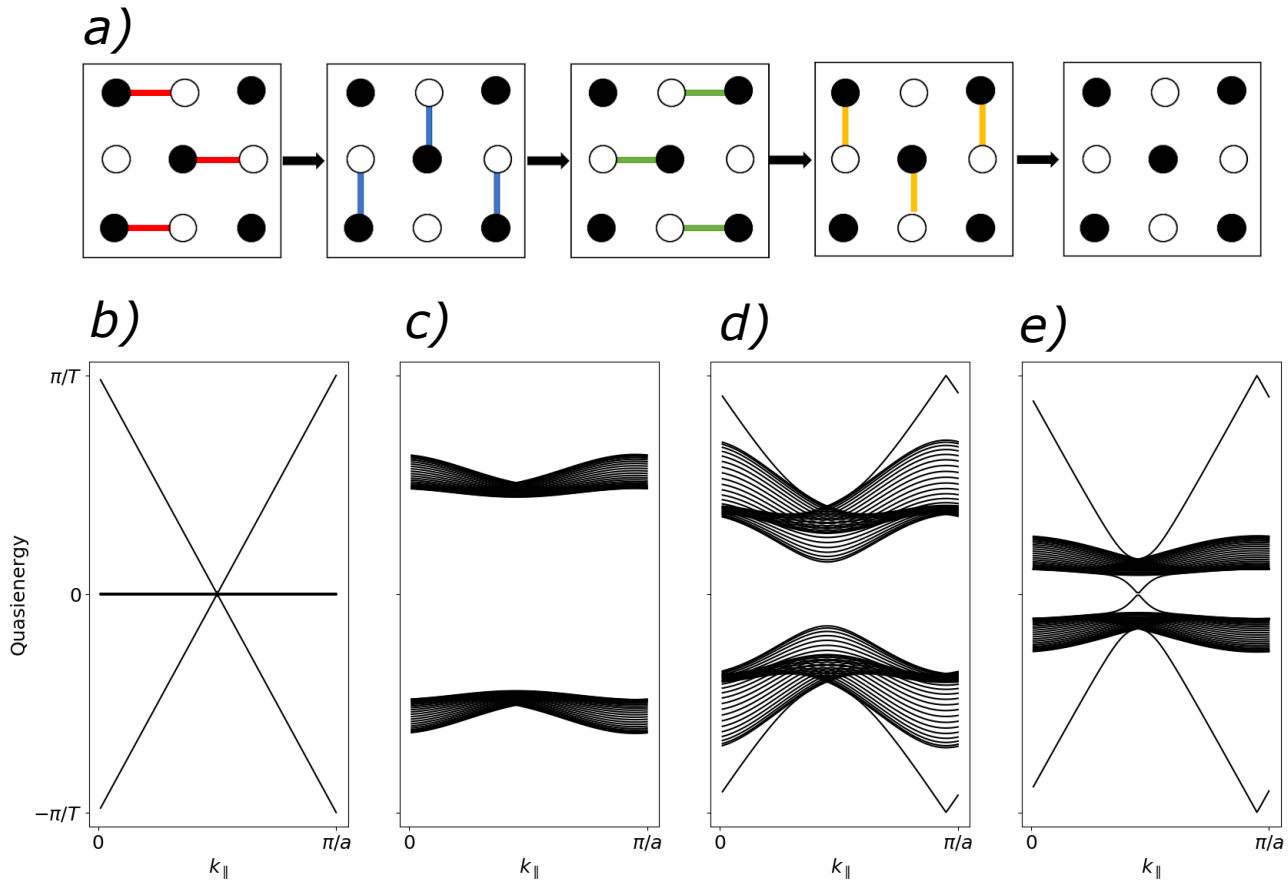

FIG. 1: In a), we show a schematic of the hopping parameters in each of the $T/5$ timesteps of one cycle of the RLBL Hamiltonian defined in the text; colored bonds indicate nonzero hopping J between the four distinct types of bonds on each timestep. In b-d), we plot the Floquet spectra in the model in a cylindrical geometry with periodic boundary conditions along one direction and finite width $M = 30$ along the other. The parameters are given by: b) $J = 2.5\pi/T$, $\delta_{AB} = 0$, c) $J = 0.5\pi/T$, $\delta_{AB} = 0.5\pi/T$, d), $J = 1.5\pi/T$, $\delta_{AB} = 0.5\pi/T$, $J = 2.5\pi/T$, $\delta_{AB} = 0.5\pi/T$. Data in this figure has been generated by the author's own code, after Rudner *et. al.*[4]

Now, consider a Floquet spectrum with a gap in some interval $[\varepsilon - \delta, \varepsilon + \delta]$. Then any Floquet eigenstates with eigenvalues in this gap must be localized on the edge - otherwise this would not be a gap in the bulk spectrum - and thus correspond with edge modes. Ideally, an invariant would be able to be defined that would tell us how many (net) chiral edge modes exist at quasienergy ε given by the bulk time evolution operator $U(\mathbf{k}, t)$.

Rudner et. al. take an approach to this by first recognizing that the invariant is straightforward in the case where $U(\mathbf{k}, T) = \mathbf{1}$ everywhere, and then proceed by reducing a more general $U(\mathbf{k}, T)$ case to the first case. If $U(\mathbf{k}, T) = \mathbf{1}$ for all $\mathbf{k}$, we can recognize this as identical to the case illustrated in Fig. 1b from the RLBL model above, where all of the bulk states have $\varepsilon = 0$ and the Floquet spectrum is gapped everywhere else, because the effective Floquet Hamiltonian $H_F = 0$. Then there should be an integer n_{edge} for each $U(\mathbf{k}, t)$ counting the number of edge modes winding around the quasienergy Brillouin zone, invariant under all smooth deformations that leave $U(\mathbf{k}, T) = \mathbf{1}$. If U has this form, then it is periodic in k_x, k_y, and t, because $U(0) = U(T) = \mathbf{1}$, so U gives a map from $S^1 \times S^1 \times S^1 \to U(N)$. This sort of map can be classified by an integer winding number given by

$$W[U] = \frac{1}{8\pi^2} \int dt dk_x dky \mathrm{Tr}(U^{-1}\partial_t U[U^{-1}\partial_{k_x} U, U^{-1}\partial_{k_y} U]) \tag{11}$$

Rudner et. al. show that this winding number $W[U]$ is equivalent to n_{edge}.

Sketching this proof, we consider a cylindrical geometry with open boundary conditions at $x = 1$ and $x = L_x$ and periodic boundary conditions in the y direction. Then let $\tilde{H}$ and $\tilde{U}$ be Hamiltonian and time evolution operators, respectively, that agree with H and U on the interior but can take any local and y-translationally invariant form on the boundary of the cylinder. Then we can describe $\tilde{H}$ and $\tilde{U}$ in mixed x and k_y space. Noting that $\tilde{U}(k_y, T)$ reduces to the identity matrix on the interior, we can

express $\tilde{U}(k_y, T)$ in block diagonal form as

$$\tilde{U}(k_y, T) = \begin{pmatrix} \tilde{U}_1(k_y) & 0 & 0 \\ 0 & \mathbf{1} & 0 \\ 0 & 0 & \tilde{U}_3(k_y) \end{pmatrix} \tag{12}$$

where $\tilde{U}_1(k_Y)$ and $\tilde{U}_3(k_y)$ describe the action of $\tilde{U}$ near the two boundaries. Then the total number of modes propagating in the y direction along both edges is given by $-\frac{1}{2\pi i}\int dk_y \mathrm{Tr}(\tilde{U}^{-1}\partial_{k_y}\tilde{U})$, which is known from previous theoretical studies on edge states[8]. Adjusting this by an operator $Q_{xx'} = g(x)\delta_{xx'}$ where $g(x) = 0$ for $x \leq L_x/3$ and $g(x) = 1$ for $x \geq 2L_x/3$, the total number of edge modes along the $x = L_x$ edge is given by

$$n_{\mathrm{edge}} = -\frac{1}{2\pi i}\int dk_y \mathrm{Tr}[\tilde{U}(k_y, T)^{-1}\partial_{k_y}\tilde{U}(k_y, T)Q] \tag{13}$$

From Eq. 13, a number of algebraic manipulations and algebra identities allow us to derive that $n_{\mathrm{edge}} = W[U]$, in particular using that Q is constant near the edges so that $\tilde{U}$ can be replaced by the bulk operator U and Fourier transforming to introduce an integral over k_x, yielding Eq. 11. Even as this derivation may not be particularly illuminating, the comparison to classification by the Chern numbers of the Floquet-Bloch bands demonstrates that this winding number is qualitatively different. Rather than depending on the Floquet states at a single moment in time, the expression $W[U]$ integrates the complete time evolution $U(\mathbf{k}, t)$ over the entire period of Floquet time T.

Now, consider the general case where $U(\mathbf{k}, T)$ is arbitrary, so that the Floquet spectra is more complex than $\varepsilon = 0$. We can achieve this by defining a family of evolution operators $\{U_s | s \in [0, 1]\}$ such that

$$U_{s=0}(\mathbf{k}, t) = U(\mathbf{k}, t), \quad U_{s=1}(\mathbf{k}, t) = U_\varepsilon(\mathbf{k}, t) \tag{14}$$

such that this interpolation maintains a gap around quasienergy ε_s that changes from $\varepsilon_{s=0} = \varepsilon$ and $\varepsilon_{s=1} = \pi/T$ and $U_\varepsilon(\mathbf{k}, T) = \mathbf{1}$. Then, because the gap doesn't close by construction, the number of edge modes of U at quasienergy ε is equivalent to the number of edge modes of U_ε at quasienergy π/T, so that following from the simpler case,

$$n_{\mathrm{edge}}(\varepsilon) = W[U_\varepsilon] \tag{15}$$

While U_ε is not general, one useful definition is

$$U_\varepsilon(\mathbf{k}, t) = \begin{cases} U(\mathbf{k}, 2t) & 0 \leq t \leq T/2 \\ V_\varepsilon(\mathbf{k}, 2T - 2t) & T/2 \leq t \leq T \end{cases} \tag{16}$$

for

$$V_\varepsilon(\mathbf{k}, t) = e^{-iH_{\mathrm{eff}}(\mathbf{k})t}, \quad H_{\mathrm{eff}}(\mathbf{k}) = \frac{i}{T}\log U(\mathbf{k}, T) \tag{17}$$

where the branch cut of the logarithm is chosen along the direction $e^{-i\varepsilon T}$, which is where the ε dependence comes in. This sort of V_ε is a "return" map connecting Floquet operator $U(\mathbf{k}, T)$ to the identity via a static effective Hamiltonian which generates a time evolution identical to $U(\mathbf{k}, T)$, so that combining them in series in this way sets $U_\varepsilon(\mathbf{k}, T) = \mathbf{1}$. The interpolation between them U_s can be written as

$$U_s(\mathbf{k}, t) = \begin{cases} U(\mathbf{k}, (1+s)t) & 0 \leq t \leq \frac{T}{1+s} \\ V_\varepsilon(\mathbf{k}, 2T - (1+s)t) & \frac{T}{1+s} \leq t \leq T \end{cases} \tag{18}$$

While slightly technical in its construction, this invariant does provide an effective classification. Applying it othe RLBL Model described above, $U(t)$ can be expressed piecewise as $U(t) = e^{-iH_1 t}$ for $t \in [0, T/5]$, $U(t) = e^{-iH_2(t-T/5)}e^{-iH_1 T/5}$ for $t \in [T/5, 2T/5]$, and so on, which reduces to a small number of exponentials of 2×2 matrices in momentum space. The return map is also given by the matrix of logarithm of $U(\mathbf{k}, T) = e^{-iH_5 T/5} \ldots e^{-iH_1 T/5}$. Combining these, we can calculate the appropriate winding numbers from Eq. 11 and 16. If we apply to the specific examples displayed in Fig. 1b-d, this winding number predicts the correct number of chiral edge states, $W_0 = W_\pi = 0$ for the small hopping case, $W_0 = 0$ and $W_\pi = 1$ for the intermediate case and $W_0 = W_\pi = 1$ for the strong hopping case. While this model has been explicitly constructed in a single-particle picture, the extension of the RLBL Model to a many-body analog through interactions is possible, though it is unclear whether these extensions can be described with a bulk topological invariant[9,11–13]. General concerns of extending single-particle Floquet systems to the many-body case are discussed below (Sec. IV).

C. Harmonic picture

The above model and classification is theoretically robust and useful for understanding "anomalous" edge states that Chern numbers alone would not predict in the Floquet-Bloch spectra. However, it's somewhat cumbersome for Floquet Hamiltonians that we might think about in the frequency, rather than time, domain. Given that experimentally, most of these time-periodic drives are implemented via laser or microwave fields, rather than any sort of time-piecewise drive like the RLBL model, it's useful to think of how this applies in the frequency domain. In the frequency domain, the Floquet theorem can be expressed on a state $\psi_{n\alpha}$ as

$$\psi_{n\alpha}(\mathbf{k}, t) = e^{-i\varepsilon_n(\mathbf{k})t}\sum_{m=-\infty}^{\infty}\phi_{n\alpha}^{(m)}(\mathbf{k})e^{im\omega t} \tag{19}$$

for $\omega = \frac{2\pi}{T}$ and $\phi_{n\alpha}^{(m)}$ satisfying a time independent eigenvalue equation:

$$\sum_{\alpha', m'}\mathcal{H}_{\alpha\alpha'}^{mm'}\phi_{n\alpha'}^{(m')} = \varepsilon_n\phi_{n\alpha}^{(m)} \tag{20}$$

This "Floquet Hamiltonian" is given by

$$\mathcal{H}^{mm'}_{\alpha\alpha'} = m\omega\delta_{\alpha\alpha'}\delta_{mm'} + \frac{1}{T}\int_0^T dt e^{-i(m-m')\omega t} H_{\alpha\alpha'}(t) \tag{21}$$

These quasienergies ε_n aren't restricted to lie in $[-\frac{\pi}{T}, \frac{\pi}{T}]$ even though it must be equivalent to that described above. Effectively, Eq. 20 is describing a repeated zone scheme along the energy axis. Now, we consider the physically realistic case where all of the time-dependence in $H(t)$ is at a single frequency, as

$$H(t) = H_0 + \Delta e^{i\omega t} + \Delta^\dagger e^{-i\omega t} \tag{22}$$

In the limit of weak driving, the Floquet Hamiltonian $\mathcal{H}^{mm'}_{\alpha\alpha'}$ is given to zeroth order in Δ as a copy of H_0 shifted up and down at integer multiples of ω. Nonzero Δ induces hopping between levels with different m levels, so that gaps open in the spectrum. The Floquet states are localized in m, meaning that they decay reapidly for $|m - m_0|\omega \gg \Lambda$, where Λ is the total bandwidth. This follows from an analogy of Wannier-Stark localization in real space, which describes how Bloch electrons localize in an electric field, to "m-space." Similarly to the electric field in that calculation, the linear contribution of $m\hbar\omega$ along the diagonal of $\mathbb{H}$ leads to their localization, though now as a function of m rather than of spatial coordinates. This allows the Floquet Hamiltonian to be truncated at large but finite M. Once this is done, the $(2M+1)\times N$ bands in the extended zone scheme can be considered as a static Hamiltonian and the standard bulk-edge correspondence applies, so that the net number of chiral edge modes in a particular gap is given by the sum of Chern numbers from all bands below that gap. This gives a more convenient way to calculate the number of chiral edge modes crossing a gap in the first (quasienergy) Brillouin zone, in that we can expand the Floquet Hamiltonian in an extended zone scheme and count the Chern numbers of the bands below the gap.

As a concrete example, Rudner et. al. consider a two-band model where $H_0(\mathbf{k}) = e(\mathbf{k}) + \mathbf{d}(\mathbf{k})\cdot\boldsymbol{\sigma}$ where the resulting bands have Chern numbers $\mathcal{C} = \pm C_0$. Assuming the drive creates a single resonance between the valence and conductance bands of H_0 simultaneously for all $\mathbf{k}$ values, then the entire band structure can be translated up and down, opening gaps between the crossings. If the resulting bands each have Chern numbers C_F and $-C_F$, due to the hybridization, then they will always have $C_0 + C_F$ chiral edge modes in the gap because there will always be a C_0 band at the bottom of the spectrum, independent of the termination. Such a model can display anomalous edge modes as a proper choice of $\mathbf{d}(\mathbf{k})$ will cause $C_0 = \pm 1$ but $C_F = 0$. Thus, all the intermediate gaps will have edge modes even though they are between bands with zero Chern number. In this picture, the anomalous states arise from the topological properties of the bands near the truncation boundaries, which retain the history of the undriven H_0 bands. Rudner et. al. comment that if more resonances are allowed (e.g. from multi-photon processes), the situation becomes more complicated, and anomalous edge states can come from an original Hamiltonian that is topologically trivial.

In Figure 2, we examine the two-band model suggested by Rudner et. al. with

$$\mathbf{d}(\mathbf{k}) = \big(a\sin(k_x), a\sin(k_y), (\mu - J) - 2b(2 - \cos(k_x) - \cos(k_y)) + J\cos(k_x)\cos(k_y)\big)$$
$$e(\mathbf{k}) = 0 \tag{23}$$

In order to investigate the edge state properties of this two-band model, we need to realize this Hamiltonian in real-space, so that it may be solved numerically in a cylindrical geometry. This can be accomplished by considering the model of two orbitals on a triangular lattice and identifying k_x and k_y with the momentum along each Bravais vector[14]. In this way, the Hamiltonian can be rewritten in terms of real-space creation and annihilation operators on a triangular lattice as

$$\begin{aligned} H = \textstyle\sum_{ij}\Big[& c^\dagger_{i+1}(i\tfrac{a}{2}\sigma_x)c_{ij} + c^\dagger_{i,j+1}(i\tfrac{a}{2}\sigma_y)c_{ij} \\ & + c^\dagger_{ij}\left(\tfrac{\mu - J - 4b}{2}\right)c_{ij} + c^\dagger_{i+1,j}(b\sigma_z)c_{ij} + c^\dagger_{i,j+1}(b\sigma_z)c_{ij} \\ & + c^\dagger_{i+1,j+1}(\tfrac{J}{4}\sigma_z)c_{ij} + c^\dagger_{i+1,j-1}(\tfrac{J}{4}\sigma_z)c_{ij} + \text{H.c.}\Big] \end{aligned} \tag{24}$$

By Fourier transforming the i coordinate in Eq. 24, corresponding to k_x, we can solve the Hamiltonian on a cylindrical geometry with periodic boundary conditions along one axis and open boundary conditions on the other. The band structure for the nondriven case is shown in Fig. 2a, for a width along the k_y direction of $M = 20$. The specific parameters chosen are $J/\mu = b/\mu = 1.5$, $a/\mu = 4$, and the energy is scaled in units of $\omega = \mu/.07$, corresponding to the drive in Fig. 2c (see below). This band structure shows a clear set of edge states crossing the bulk band gap, corresponding to a single chiral mode on each edge of the cylinder. The existence of these edge states shows that the unperturbed bands have Chern number $C_0 = \pm 1$, due to the usual bulk-boundary correspondence, as there's no Floquet dynamics at this point. This can also be checked explicitly. Next, in Fig. 2b-c, we plot the spectrum of the Floquet Hamiltonian as defined in Eq. 21 above, where the driving term introduced to the static Hamiltonian is $\Delta = \Delta_0\sigma_z\cos(\omega t)$. We set $\Delta_0/\mu = 1$ in both plots; their only difference is that in the Fig. 2b, $\omega = \frac{\mu}{.05}$ and in Fig. 2c, $\omega = \frac{\mu}{.07}$. In Fig. 2b, ω is large enough that the bands translated up and down by ω just hybridize and open gaps around $k_\parallel = \pm\pi/a$ and it's straightforward to identify the individual copies of the static band structure shown in Fig. 2a with $m = -1$, $m = 0$, and $m = +1$ in the extended, Floquet band structure. Because the opened gaps at the $k_\parallel = \pm\frac{\pi}{a}$ are quite small, it's difficult to see the edge states crossing these gaps. Alternatively, in Fig. 2c, the smaller drive frequency leads to larger hybridization between adjacent m in the Floquet Hamiltonian, and the edge states

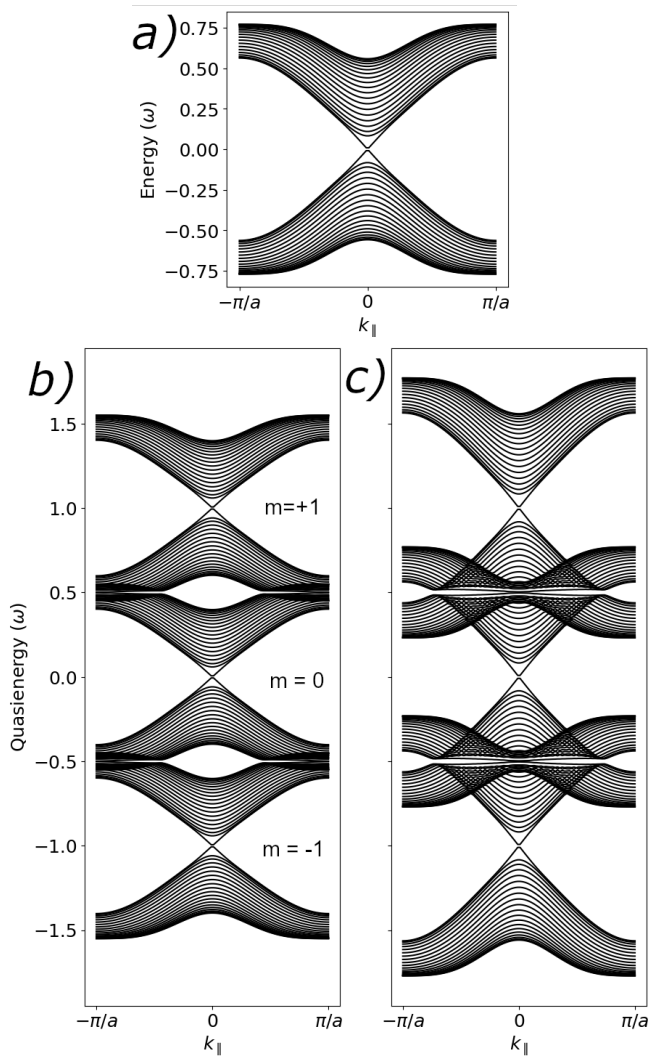

FIG. 2: In a), we show the band structure of two-band static Hamiltonian H_0 (see Eq. 23, 24). The band structure is solved numerically in a cylindrical geometry with periodic boundary conditions in one direction and $M = 20$ sites in the other direction. The parameters chosen are $J/\mu = b/\mu = 1.5$ and $a/\mu = 4$. A pair of chiral edge states can be seen crossing the bulk band gap; this static band structure is topologically nontrivial with Chern numbers $C_0 = \pm 1$ of each band. In b-c), we plot the Floquet spectra via numerical solution of the Floquet Hamiltonian as defined in Eq. 21, truncated at $m = \pm 1$. The drive is given by $\Delta_0 \sigma_z \cos(\omega t)$ where $\Delta_0/\mu = 1$. In b), $\omega = \frac{\mu}{.05}$ and in c), $\omega = \frac{\mu}{.07}$. To zeroth order, the Floquet Hamiltonian results in repeated copies of the band structure shifted up and down by ω, though higher orders of perturbation theory lead to gaps opening where these bands cross (e.g., at $\varepsilon = \pm 0.5$ in the Floquet spectra). Even though the Floquet bands in the middle of this spectrum have $C_F = 0$, chiral edge states are still observed traversing these gaps. Data in this figure has been generated by the author's own code, after Rudner *et. al.*[4]

crossing these opened gaps are apparent. Due to the bulk-edge correspondence, these internal Floquet bands must have Chern numbers $C_F = 0$, and yet they still exhibit edge states at the gaps between them. Through this toy model, the consistency of anomalous edge states with harmonic Floquet drives is apparent, and, conveniently, the number of edge states in a given gap can be computed in a much more straightforward manner than the general formula (Eq. 15).

IV. RELEVANCE TO PHYSICAL SYSTEMS

This single-particle picture of Floquet dynamics in a completely closed system allows for a detailed theoretical understanding of topological edge modes and predictions of multiple types of induced, nonequilibrium topological phases. A number of recent experiments, such as in cold-atomic gases and solid-state systems have realized these phenomena[15,16]. In understanding how the single-particle, closed system picture extends to physical systems, we consider how general concepts from many-body systems might apply.

A recent review from Harper et. al.[9] discusses some of the implications of many-body interactions on the topological Floquet systems. In principle, a closed, interacting Floquet system should heat to infinite temperature. Without energy conservation, entropy is always maximized by the infinite temperature state[17–19]. In this trivial case, any interesting topological properties would be essentially unmeasurable under the thermalization to a completely trivial state. However, there are some possibilities that avoid devolution into the infinite-energy state: many-body localization (MBL), prethermalization, and cooling, each discussed in further detail below.

A. Floquet-MBL

In analogy to the way that static, highly interacting, closed systems can be classified as thermalizing or MBL, one might expect that this limit for a driven system also leads to the possibility of localized phase. Following the l-bit definition of MBL in time-independent systems, in the limit of large enough disorder, localized l-bit operators τ_i^z can be defined such that $[U(T), \tau_i^z] = 0$. A conceptual way to think of these operators are that each one exchanges energy (absorbing and transfering it back) to the driving field over an evolution $U(T)$ but no energy is exchanged between the local oscillators. Making this definition more formal requires extending eigenstate thermalization hypothesis (ETH), the hypothesis as to how closed quantum systems thermalize as opposed to localize, to Floquet eigenstates. A number of recent theoretical and experimental works suggests the existence of Floquet-MBL phases, including those which have their own rich phase structure well beyond the scope of this

paper[19–24].

One feature that's worth commenting on is that MBL phases can, in some cases, be incompatible with the requirement of delocalized states that arise from nontrivial topology. The existence of delocalized states in equilibrium topological phases, connected with the chiral modes that appear on the system boundaries, cannot be localized by disorder. These delocalized states will generically destabilize MBL phases at any energy density[25,26]. In the logical extension Floquet topological case, this suggests that the Floquet bands carrying non-trivial topological indices, such as those in Type I Floquet topological phases described above, will likely not exhibit stable MBL-Floquet phases even in a limit of high disorder. However, the Type II phases where trivial Floquet bands exist alongside anomalous edge modes should be consistent with an MBL phase, as these bands do not include delocalized bulk states[25].

B. Prethermalization

A second manner in which heating may be avoided is the possibility of "prethermalization," that heating to the steady state will take $\mathcal{O}(e^{J/T})$ time in some physically relevant energy scale J. This is a temporal analog of how Anderson localization is difficult to observe in a clean $d = 2$ system where, with weak enough disorder, the localization length may be parametrically large compared to the measurable system size. Many of the early experiments probing for edge states in Floquet systems purposefully try and examine this regime by performing their measurements on ultrafast length scales, long before the system reaches any sort of steady state[16]. Generally, heating rates will be small if the drive frequency is much larger than the relevent energy scales in the problem, such as the single-particle bandwidth. But in any real physical system, higher bands will always be present. However, this regime can still be useful. If $\hbar\omega$ is much smaller than the gap separating higher energy bands from bands closer to the Fermi level, then many photons need to be absorved to excite into a high-energy state, so that these excitations are exponentially suppressed, allowing the "finite" bandwidth to be recovered to a certain extent. The precise nature of the length of time that a quasisteady, prethermalized state may exist is dependent on details of the system being measured and periodicity of the drive, but in certain limits it is likely to be long-lived. Regardless, systems of ultrafast measurement are appropriate for ensuring that these Floquet systems are in something like these "prethermal" states by avoiding any questions and concerns about long-time behavior.

C. Open Systems

A third way that Floquet systems generically avoid heating to infinite temperature, trivial states is due to their existence as open systems - particularly in solid-state systems. Due to coupling to the environment and external baths, the steady state will be reached by balancing the heating from the drive with energy and entropy exchanged with the baths. These can be bosonic or fermionic baths, due to any number of physical parameters such as phonons or external leads. Because this is happening out of equilibrium for a Floquet system, the steady-state is not dependent on a small number of macroscopic parameters as in the usual, equilibrium case (e.g. temperature, chemical potential, and so on). The precise steady state will depend sensitively on the microscopics of both the bath and the coupling to the bath. A number of recent theoretical studies have addressed in specific systems whether these sorts of topological Floquet states will be stable as open systems. For example, Dehghani et. al. simulated the nonequilibrium Floquet occupation of graphene driven by circularly polarized light in the presence (and absence) of phonons at a finite temperature[27]. They conclude that there might be a regime where the quantized transport from edge states remains, but only in specific parameter regimes, such as low phonon bath temperature and relatively high frequency drive to avoid excited photocarriers. However, some of these issues can be ignored at short time scales as a Floquet drive is turned "on", as the time-scales of electron-phonon coupling are somewhat slower than the electronic dynamics. Regardless, in the general case, these open systems (and the extent to which Floquet chiral edge states may or may not survive with the addition of dissipation) remain an open question.

V. CONCLUSION

While the theory of Floquet edge states is relatively well-developed in the single-particle picture, there are numerous open experimental and theoretical questions. For instance, even though topological Floquet edge states have been seen in multiple types of experiments, the more physically novel "Type II" phases in a single-particle system hasn't been shown in the lab, though more general "Type II" phases in a many-body context have been seen[28,29]. These single-particle "Type II" phases should have particular experimental signatures[30] and are intrinsically dynamical phases. Further, beyond the ultrafast regime, there are a number of open theoretical questions that can be asked about these sorts of systems. For example, the time dynamics of thermalization in the presence of dissipation and the topological properties that might exist in certain Floquet-MBL phases are relatively little understood and studied. The interplay of topological

and inherently nonequilibrium states of matter should continue to be an active field of research, particularly as experiments can begin to address some of these questions.

[1] X.-L. Qi and S.-C. Zhang, Rev. Mod. Phys. **83**, 1057 (2011), URL https://link.aps.org/doi/10.1103/RevModPhys.83.1057.

[2] M. Z. Hasan and C. L. Kane, Rev. Mod. Phys. **82**, 3045 (2010), URL https://link.aps.org/doi/10.1103/RevModPhys.82.3045.

[3] M. König, S. Wiedmann, C. Brüne, A. Roth, H. Buhmann, L. W. Molenkamp, X.-L. Qi, and S.-C. Zhang, Science **318**, 766 (2007), ISSN 0036-8075, https://science.sciencemag.org/content/318/5851/766.full.pdf, URL https://science.sciencemag.org/content/318/5851/766.

[4] M. S. Rudner, N. H. Lindner, E. Berg, and M. Levin, Phys. Rev. X **3**, 031005 (2013), URL https://link.aps.org/doi/10.1103/PhysRevX.3.031005.

[5] C. Kane, in *Topological Insulators*, edited by M. Franz and L. Molenkamp (Elsevier, 2013), vol. 6 of *Contemporary Concepts of Condensed Matter Science*, chap. 1, p. i, URL http://www.sciencedirect.com/science/article/pii/B9780444633149000123.

[6] R. B. Laughlin, Phys. Rev. B **23**, 5632 (1981), URL https://link.aps.org/doi/10.1103/PhysRevB.23.5632.

[7] B. I. Halperin, Phys. Rev. B **25**, 2185 (1982), URL https://link.aps.org/doi/10.1103/PhysRevB.25.2185.

[8] T. Kitagawa, E. Berg, M. Rudner, and E. Demler, Phys. Rev. B **82**, 235114 (2010), URL https://link.aps.org/doi/10.1103/PhysRevB.82.235114.

[9] F. Harper, R. Roy, M. S. Rudner, and S. L. Sondhi, Annual Review of Condensed Matter Physics **11**, 345 (2020), URL https://www.annualreviews.org/doi/abs/10.1146/annurev-conmatphys-031218-013721.

[10] D. N. Basov, R. D. Averitt, and D. Hsieh, Nature Materials **16**, 1077 (2017), ISSN 1476-4660, URL https://doi.org/10.1038/nmat5017.

[11] H. C. Po, L. Fidkowski, T. Morimoto, A. C. Potter, and A. Vishwanath, Phys. Rev. X **6**, 041070 (2016), URL https://link.aps.org/doi/10.1103/PhysRevX.6.041070.

[12] F. Harper and R. Roy, Phys. Rev. Lett. **118**, 115301 (2017), URL https://link.aps.org/doi/10.1103/PhysRevLett.118.115301.

[13] F. Nathan, D. Abanin, E. Berg, N. H. Lindner, and M. S. Rudner, Phys. Rev. B **99**, 195133 (2019), URL https://link.aps.org/doi/10.1103/PhysRevB.99.195133.

[14] D. Sticlet, F. Piéchon, J.-N. Fuchs, P. Kalugin, and P. Simon, Phys. Rev. B **85**, 165456 (2012), URL https://link.aps.org/doi/10.1103/PhysRevB.85.165456.

[15] N. Fläschner, B. S. Rem, M. Tarnowski, D. Vogel, D.-S. Lühmann, K. Sengstock, and C. Weitenberg, Science **352**, 1091 (2016), ISSN 0036-8075, https://science.sciencemag.org/content/352/6289/1091.full.pdf, URL https://science.sciencemag.org/content/352/6289/1091.

[16] J. W. McIver, B. Schulte, F.-U. Stein, T. Matsuyama, G. Jotzu, G. Meier, and A. Cavalleri, Nature Physics **16**, 38 (2020), ISSN 1745-2481, URL https://doi.org/10.1038/s41567-019-0698-y.

[17] A. Lazarides, A. Das, and R. Moessner, Phys. Rev. E **90**, 012110 (2014), URL https://link.aps.org/doi/10.1103/PhysRevE.90.012110.

[18] L. D'Alessio and M. Rigol, Phys. Rev. X **4**, 041048 (2014), URL https://link.aps.org/doi/10.1103/PhysRevX.4.041048.

[19] P. Ponte, A. Chandran, Z. Papi, and D. A. Abanin, Annals of Physics **353**, 196 (2015), ISSN 0003-4916, URL http://www.sciencedirect.com/science/article/pii/S0003491614003212.

[20] P. Bordia, H. Lüschen, U. Schneider, M. Knap, and I. Bloch, Nature Physics **13**, 460 (2017), ISSN 1745-2481, URL https://doi.org/10.1038/nphys4020.

[21] P. Ponte, Z. Papić, F. m. c. Huveneers, and D. A. Abanin, Phys. Rev. Lett. **114**, 140401 (2015), URL https://link.aps.org/doi/10.1103/PhysRevLett.114.140401.

[22] A. Lazarides, A. Das, and R. Moessner, Phys. Rev. Lett. **115**, 030402 (2015), URL https://link.aps.org/doi/10.1103/PhysRevLett.115.030402.

[23] D. A. Abanin, W. D. Roeck], and F. Huveneers, Annals of Physics **372**, 1 (2016), ISSN 0003-4916, URL http://www.sciencedirect.com/science/article/pii/S000349161630001X.

[24] V. Khemani, A. Lazarides, R. Moessner, and S. L. Sondhi, Phys. Rev. Lett. **116**, 250401 (2016), URL https://link.aps.org/doi/10.1103/PhysRevLett.116.250401.

[25] M. S. Rudner and N. H. Lindner, Nature Reviews Physics **2**, 229 (2020), ISSN 2522-5820, URL https://doi.org/10.1038/s42254-020-0170-z.

[26] R. Nandkishore and A. C. Potter, Phys. Rev. B **90**, 195115 (2014), URL https://link.aps.org/doi/10.1103/PhysRevB.90.195115.

[27] H. Dehghani, T. Oka, and A. Mitra, Phys. Rev. B **90**, 195429 (2014), URL https://link.aps.org/doi/10.1103/PhysRevB.90.195429.

[28] S. Choi, J. Choi, R. Landig, G. Kucsko, H. Zhou, J. Isoya, F. Jelezko, S. Onoda, H. Sumiya, V. Khemani, et al., Nature **543**, 221 (2017), ISSN 1476-4687, URL https://doi.org/10.1038/nature21426.

[29] J. Zhang, P. W. Hess, A. Kyprianidis, P. Becker, A. Lee, J. Smith, G. Pagano, I.-D. Potirniche, A. C. Potter, A. Vishwanath, et al., Nature **543**, 217 (2017), ISSN 1476-4687, URL https://doi.org/10.1038/nature21413.

[30] A. Kundu, M. Rudner, E. Berg, and N. H. Lindner, Phys. Rev. B **101**, 041403 (2020), URL https://link.aps.org/doi/10.1103/PhysRevB.101.041403.